



In Silico Evaluation of Natural Antiviral Compounds Targeting the RBM of SARS-CoV-2 Spike Glycoprotein

Ilyes Zatla* and Lamia Boublenza

Laboratory of Microbiology applied to the Food industry, Biomedical and the Environment, Faculty of Natural and Life Sciences, Earth and Universe Sciences, Department of Biology, University of Tlemcen, Algeria.

ARTICLE INFO

Article history:

Received 19 August 2023

Revised 10 September 2023

Accepted 07 October 2023

Published online 01 November 2023

Copyright: © 2023 Zatlá and Boublenza. This is an open-access article distributed under the terms of the [Creative Commons Attribution License](https://creativecommons.org/licenses/by/4.0/), which permits unrestricted use, distribution, and reproduction in any medium, provided the original author and source are credited.

ABSTRACT

Emerging in Wuhan in December 2019, Severe Acute Respiratory Syndrome Coronavirus 2 (SARS-CoV-2) has triggered a devastating global pandemic. In response to this crisis, considerable efforts have been dedicated to developing preventive and therapeutic approaches, including investigations into natural products that hold promise in combatting COVID-19. This study utilized computational methods to screen and identify six potential natural antiviral compounds with demonstrated efficacy against the SARS-CoV-2 spike glycoprotein. Molecular docking simulations were employed to predict and analyze the binding interactions between these selected natural compounds and the target protein. Factors such as binding affinity, interaction patterns, and structural compatibility within active sites were taken into account. The results revealed that some of the molecules exhibited positive binding, others didn't bind at all, with possible interactions between them and the target protein. The computational evaluation obtained for these compounds call for further investigation to evaluate their potential as Spike glycoprotein inhibitors, presenting potential benefits in COVID-19 treatment. These findings contribute to the discovery of novel natural antiviral compounds for SARS-CoV-2, offering valuable leads for subsequent experimental validation and future drug design strategies in the ongoing battle against COVID-19.

Keywords: Severe Acute Respiratory Syndrome Coronavirus 2, COVID-19, Spike glycoprotein, Antiviral, Biomolecules, Molecular dynamics.

Introduction

Since its initial detection in Wuhan in December 2019, severe acute respiratory syndrome coronavirus 2 (SARS-CoV-2) has caused more than 641 million cases of COVID-19 and led to the loss of over 6.6 million lives as of December 2022. This virus has demonstrated remarkable effectiveness as a human pathogen and has shown adaptability in infecting various mammalian species. It accomplishes this by utilizing different mammalian angiotensin-converting enzyme 2 (ACE2) membrane proteins to gain entry into host cells.¹⁻³ The extensive impact of the COVID-19 pandemic has driven significant efforts to develop effective prevention and treatment strategies. Notably, these endeavors have resulted in the rapid development of multiple successful vaccines within an unprecedented timeframe. Additionally, several potential treatments have undergone evaluation in clinical trials, with a few being approved for use. Among the emerging anti-SARS-CoV-2 agents, two categories stand out: one targets viral proteins, particularly viral enzymes, to disrupt the viral life cycle, while the other focuses on host proteins involved in the viral life cycle, such as receptors responsible for viral entry.^{4,5}

Natural products continue to hold tremendous promise and provide a practical approach to the fight against pathogenic agents. Extensive research has been conducted on bioactive natural products derived from medicinal plants, animal sources, and marine organisms.

These natural products have undergone rigorous studies in various settings, including in vitro experiments, animal models, and clinical trials. They have emerged as significant contenders in COVID-19 therapy, contributing to ongoing efforts to combat the pandemic. However, it is essential to acknowledge that drug research and development is a time-consuming process. Despite some encouraging clinical results, the development of small-molecule inhibitors still faces substantial challenges and requires further advancements.^{5,6}

The main objective of this study is to employ in silico methods to comprehensively investigate and identify potential natural antiviral compounds from various sources, with a specific focus on their efficacy against SARS-CoV-2. By utilizing computational techniques, a wide range of natural compounds derived from diverse sources, such as fungi, algae, and plants, will be screened to evaluate their potential antiviral activity against critical viral targets, including the Spike protein, Main Protease, and RNA-dependent RNA polymerase (RDRP). Molecular docking simulations will be performed to predict and analyze the binding interactions between the selected natural compounds and the target proteins. Key factors, such as binding affinity, interaction patterns, and structural compatibility within the active sites, will be carefully considered. Furthermore, the chemical diversity and structural characteristics of the identified natural compounds will be assessed to uncover potential molecular scaffolds or functional groups that contribute to their antiviral activity. To validate the computational findings, a comparison will be made between the predicted antiviral properties and information available in the relevant literature and ADEMETS (Absorption, Distribution, Metabolism, Excretion, Toxicity) reports. The ultimate goal of this study is to make significant contributions to the discovery of novel natural antiviral compounds specifically targeting SARS-CoV-2. The findings will serve as potential leads for subsequent experimental validation and provide a foundation for future drug design strategies in the ongoing battle against COVID-19.

*Corresponding author. E mail: ilyes.zatla@univ-tlemcen.dz
Tel: +213-540-315422

Citation: Zatlá I and Boublenza L. *In Silico* Evaluation of Natural Antiviral Compounds Targeting the RBM of SARS-CoV-2 Spike glycoprotein. Trop J Nat Prod Res. 2023; 7(10):4273-4283. <http://www.doi.org/10.26538/tjnpr/v7i10.23>.

Official Journal of Natural Product Research Group, Faculty of Pharmacy, University of Benin, Benin City, Nigeria

Materials and Methods

In this study, we conducted an analytical *in silico* study to investigate the binding interactions between six natural molecules derived from different natural organisms against a target protein of the SARS-CoV-2 virus. The study employed computational docking techniques to predict and analyze the binding modes and affinities of the ligands within the target protein active sites, aiming to identify potential ligand-receptor interactions and gain insights into the binding mechanisms.

ADMET characteristics profiling validation was utilized using the pkCSM package to identify molecules with favorable properties for oral bioavailability and potential as medications within the body, to predict the toxic effects of compounds, while also assessing their drug-like physical and chemical properties.

Preparation of Ligand Structures

In an era where antiviral research is of paramount importance. Nature, as a rich repository of bioactive compounds, presents an intriguing opportunity to discover novel antiviral molecules. Six natural molecules were chosen according to their antiviral characteristics from the literature, where we included two plant-based molecules,^{7, 8} Cannabidiol (from *Cannabis sativa*) and Capsaicin (from *Capsicum annuum*), two fungi-based molecules,⁹ Cladosin C (from microfungi *Cladosporium sphaerospermum*) and Rhodatin (from macrofungi *Rhodotus palmatus*), also, two algae-based molecules,¹⁰ Astaxanthin (from green microalgae *Haematococcus pluvialis*) and Kappa-Carrageenan (from red marine macroalgae *Kappaphycus alvarezii*) were selected as ligands, by selecting diverse organisms, we endeavor to demonstrate that antiviral agents may be found ubiquitously, reinforcing the notion that nature's pharmacopeia remains a valuable resource in the quest for antiviral therapeutics. The structures of these six molecules were retrieved from the PubChem database, and further processed and optimized using ChemDraw and

Chimera software.

ChemDraw was employed for drawing and editing the initial ligand structures, which facilitated the accurate representation of the ligands based on the available information from PubChem.

UCSF Chimera¹¹ was utilized to optimize the ligand structures, including energy minimization and geometry optimization, leading to more reliable and physicochemically reasonable conformations.

Preparation of Receptor Structures

The structure of the Spike glycoprotein was retrieved from the PDB database and saved as PDB files.

The catalytic domains were selected for inhibitor docking of inhibitors against the SARS-CoV-2 target using PyMol (The PyMOL Molecular Graphics System, Version 1.2r3pre, Schrödinger, LLC), as well as according to literature.¹²

Spike glycoprotein RBM (receptor binding motif) of the SARS-CoV-2 virus is a crucial part of the virus responsible for binding to the ACE2 receptor on the host cell, facilitating viral entry. Its catalytic sites are: CYS336, CYS361, CYS379, CYS432, CYS391, CYS525, CYS480, CYS488. These disulfide bonds are essential for maintaining the overall structure and stability of the spike glycoprotein, while maintaining its integrity, allowing the virus to enter and infect the host cells.

Grid Generation

To define the binding sites for docking, grids were generated around the active sites of the SARS-CoV-2 proteins, namely the RBM of the spike protein. The grid parameters, including size, spacing, and center coordinates, were set using the AutoGrid module of AutoDock.¹³

Docking Protocol

All the retrieved compounds were docked using the selected catalytic site of the three-dimensional structure. The ligands were prepared by adding polar hydrogens, merging nonpolar hydrogens, and assigning partial charges using AutoDock Tools.¹⁴ The prepared ligands were then docked into the binding sites of the SARS-CoV-2 proteins using AutoDock Vina.¹⁵ Multiple docking runs were conducted to explore different ligand conformations and orientations within the binding sites.

Post-Docking Analysis

After the docking simulations, the resulting poses were analyzed to identify potential ligand-receptor interactions and select the most favorable binding conformations. The docking results were visually inspected and analyzed using molecular visualization software AutoDock Tools. The binding poses were assessed based on their binding energies, ligand-receptor interactions, and conformational fit within the active site.

Molecular dynamics simulations

Schrödinger LLC Desmond software^{16, 17} was employed for performing molecular dynamics (MD) simulations for a duration of 100 nanoseconds.¹⁸ Prior to the MD simulation, a crucial step involved the protein-ligand docking, which predicted the static binding position of the ligand molecule at the active site of the protein as mentioned before.¹⁹ MD simulations, incorporating Newton's classical equation of motion, simulate the movement of atoms over time and provide insights into the dynamic behavior and ligand-binding status in a physiological environment.²⁰

The ligand-receptor complex was preprocessed using Maestro's Protein Preparation Wizard, which performed optimization, minimization, and filling of any missing residues as necessary. The system was constructed using the System Builder tool. The MD simulation employed the TIP3P (Intermolecular Interaction Potential 3 Points Transferable) solvent model, utilizing an orthorhombic box with a temperature of 300 K, pressure of 1 atm, and the OPLS_2005 force field.²¹ To maintain physiological conditions, counter ions were introduced, and the system was neutralized using 0.15 M sodium chloride. Before the simulation, the models were equilibrated, and trajectories were recorded at regular intervals of 100 ps for subsequent analysis and inspection.

Results and Discussion

ADMET characteristics

Table 1 presents the ADMET properties of the six chosen molecules. These properties meet the criteria set by Lipinski's rule, including an additional condition on the number of rotatable bonds, indicating favorable pharmacokinetic permeability and oral bioavailability.^{22, 23}

As a target for SARS-CoV-2, spike glycoprotein (PDB ID. 6VXX) RBM was chosen to assess the binding affinity and stability of the 6 ligands against this target. Both protein and ligands RMSD plots showed that rhodatin and Kappa-Carrageenan are unable to bind to the spike glycoprotein pocket at all (Figure 1.E and 1.F) according to their structural mismatch represented by the Protein-Ligand RMSD. On the other hand, cannabidiol seems to be the best hit to spike glycoprotein upon binding a stable RMSD; fluctuating between 9 and 12 Å^o in the first 50 ns and 12 to 15 Å^o during the last 50 ns which is an acceptable range (Figure 1.B).²⁴ For spike-astaxanthin and spike-capsaicin complexes, the complexes reach a steady binding mode with a good binding affinity after about 25 ns and 15 ns, respectively (g. 1.A and 1.C). This was not the case with Cladosin C which showed a remarkable very high fluctuation range during more than 75% of the simulation until it managed to bind to spike glycoprotein active pocket.

Protein-ligand complexes stability were studied via understanding the formed protein ligand complexes. Figure 2.B showed that 9 residues in spike glycoprotein have the capacity to engage in various types of interactions with astaxanthin in more than 30% of the simulation time via either H-bond, water bridge or hydrophobic interactions. These residues are Ser 94, Glu 96, Ile 101, Trp 104, Val 126, Ile 128, Tyr 170, Arg 190 and Pro 230. Among these interactions, only Val 126, Ile 128, and Tyr 170 are the only residues that kept their interactions in almost all the MD simulation, according to which residues interact with the ligand in each trajectory frame represented in Figure 2.D where Some residues make more than one specific contact with the ligand, which is represented by a darker shade of orange, according to the scale to the right of the plot. Glu 96 and Ile 101 formed their interactions with astaxanthin after around 20 ns of the trajectory then these interactions were broken around 55 ns and then reformed again at 85 ns (Figure 2.D). Consequently, the average total number of contacts was 6 (Figure 2.C). The illustrative ligand diagram displayed only the residues capable of

forming interactions with an interaction fraction exceeding 0.3. As a result, it revealed four primary interactions, including a hydrogen bond with Ile 101, a water bridge with Glu 96, and 2 hydrophobic interactions with Ile 128 and Tyr 170 (Figure 2.E).

Cannabidiol-Spike complex RMSDs plots (Figure 1.B) suggested that it is the most stable complex with the best binding affinity according to the chart. Also, this complex RMS fluctuation showed that the residues involved in the interaction; marked with green-colored vertical bars, are very steady (Figure 3.A). Three amino acids are responsible for this interaction; a H-bond via Asn 121, a Pi-cation interaction via Arg 190 and a hydrophobic interaction via Phe 192 (Figure 3.B and 3.E). The H-bond formed between Asn 121 and cannabidiol is reported to be the most stable interaction while the Pi-cation interaction formed with Arg 190 short lived after around 70 ns. On the other hand, the formed hydrophobic interaction is discontinuous during the whole simulation (Figure 3.D). Much like cannabidiol, capsaicin exhibited stable binding when in complex with the spike glycoprotein. The complex RMSF shows low fluctuations at the binding site residues (Figure 4.A). Only 2

residues were involved in this significant binding interaction; Trp 104 and Ser 205 forming hydrophobic interaction and H-bonding, respectively (Figure 4.B and 4.E). Both interactions were not continuously formed throughout the 100 ns trajectory frames but the H-bond formed by Ser 205 seems to be stronger (Figure 4.D).

Although Cladosin C RMSD shows high fluctuation indicating its instability when bound to spike glycoprotein (Figure 1.D), it managed to interact with Lys 964 in about 50% of the simulation time (Figure 5). When rhodatin binds to SARS-CoV-2 glycoprotein, it interacts with 5 residues in the active pocket via Tyr 38 (Pi-Pi stacking), Asp 40 (H-bond), Glu 224 (H-bond), Tyr 279 (water bridge and Asn 282 (H-bond) (Figure 6.B and 6.E). Spike glycoprotein RMSF highlights these residues as the least fluctuating ones and marked them in green bars (Figure 6.A). Asp 40 was able to interact with the ligand with 2 types of interactions (water bridge and H-bond). That is why it is marked with a darker orange shade in figure 6.D. Similarly, a dark shade was observed with Tyr 38 with also interacts with the ligand via water bridge and hydrophobic interaction (Figure 6.D).

Table 1: ADMET characteristics of the six biomolecules predicted by pkSCM package

Carrageenan	Rhodatin	Cladosin C	Capsaicin	Cannabidiol	Astaxanthin	Molecule
368.368	398.455	250.298	305.418	314.469	598.868	MOL_WEIGHT
3.06828	3.4701	1.56907	3.7896	5.8465	9.1294	LOGP
5	1	4	9	6	11	ROTATABLE_BONDS
5	6	4	3	2	4	ACCEPTORS
3	3	4	2	2	2	DONORS
154.397	169.004	106.029	132.74	140.109	265.976	SURFACE_AREA
-3.011	-3.635	-2.147	-3.842	-3.396	-6.127	Water solubility
524	562	-256	1.338	956	827	Caco2 permeability
81.971	91.746	72.937	92.836	91.534	93.641	Intestinal absorption (human)
-2.894	-2.827	-2.755	-3.133	-2.764	-2.659	Skin Permeability
Yes	Yes	No	Yes	Yes	Yes	P-glycoprotein substrate
No	Yes	No	No	Yes	No	P-glycoprotein I inhibitor
No	Yes	No	No	No	Yes	P-glycoprotein II inhibitor
0.59	42	-0.37	142	618	-784	VDss (human)
248	0.04	474	115	0.04	0	Fraction unbound (human)
-1.025	-802	-939	-411	7	395	BBB permeability
-2.962	-2.327	-3.421	-2.328	-1.293	-1.383	CNS permeability
No	No	No	No	No	No	CYP2D6 substrate
No	Yes	No	Yes	No	Yes	CYP3A4 substrate
No	No	No	Yes	Yes	No	CYP1A2 inhibitor
No	No	No	No	No	No	CYP2C19 inhibitor
No	No	No	Yes	No	No	CYP2C9 inhibitor
No	No	No	No	No	No	CYP2D6 inhibitor
No	No	No	Yes	No	No	CYP3A4 inhibitor
218	319	332	1.294	1.165	849	Total Clearance
No	No	No	No	No	No	Renal OCT2 substrate
No	No	No	No	No	No	AMES toxicity
-317	-759	257	302	-202	-424	Max. tolerated dose (human)
No	No	No	No	No	No	hERG I inhibitor
No	No	No	Yes	Yes	No	hERG II inhibitor
1.953	2.61	2.726	2.566	2.35	4.061	Oral Rat Acute Toxicity (LD50)
1.472	1.909	1.31	1.85	2.517	2.28	Oral Rat Chronic Toxicity (LOAEL)
Yes	No	No	No	No	No	Hepatotoxicity
No	No	No	No	No	No	Skin Sensitisation
392	289	61	1.511	893	313	T. Pyriformis toxicity
2.093	92	2.313	0.21	-858	-2.682	Mimow toxicity

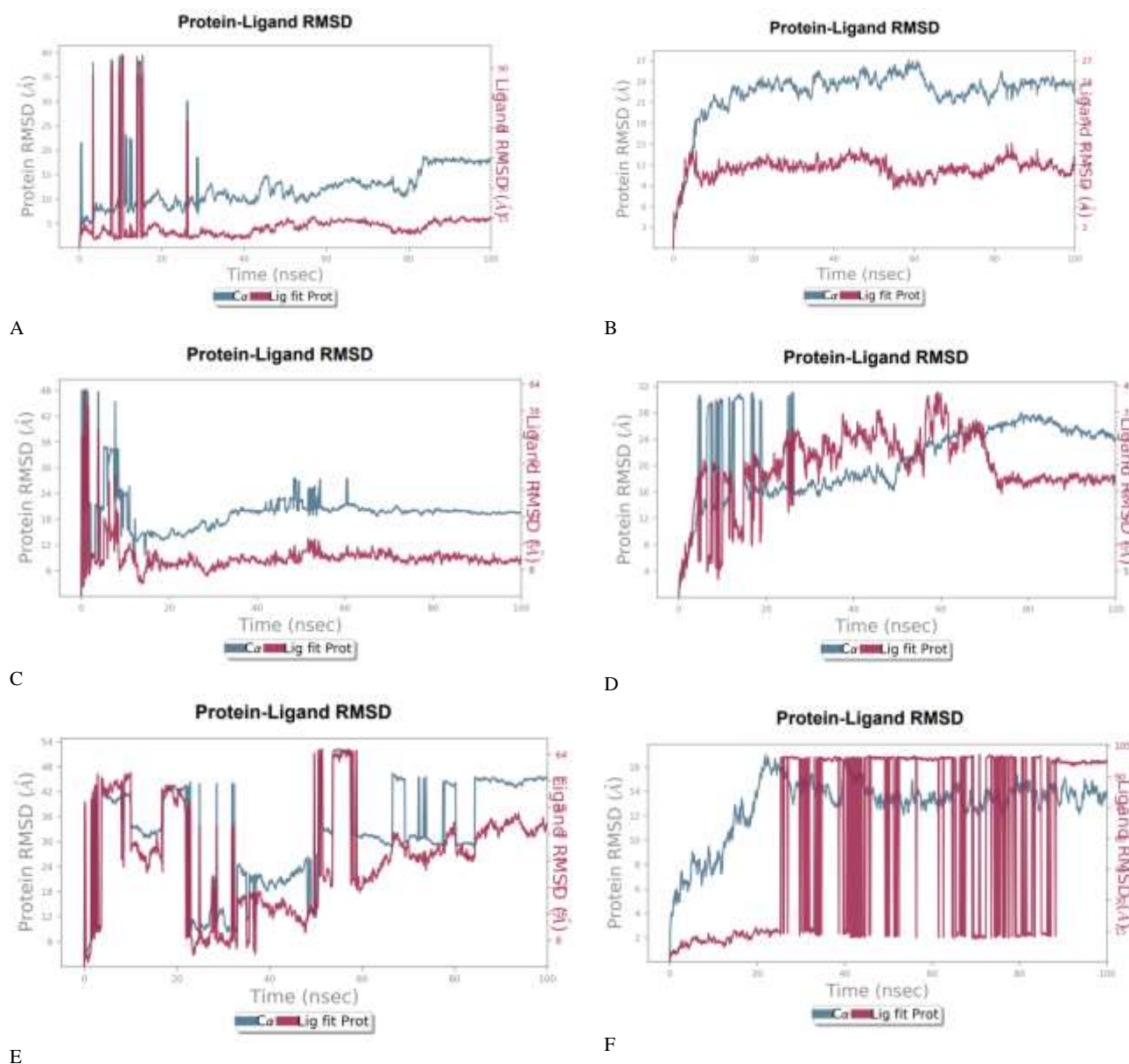
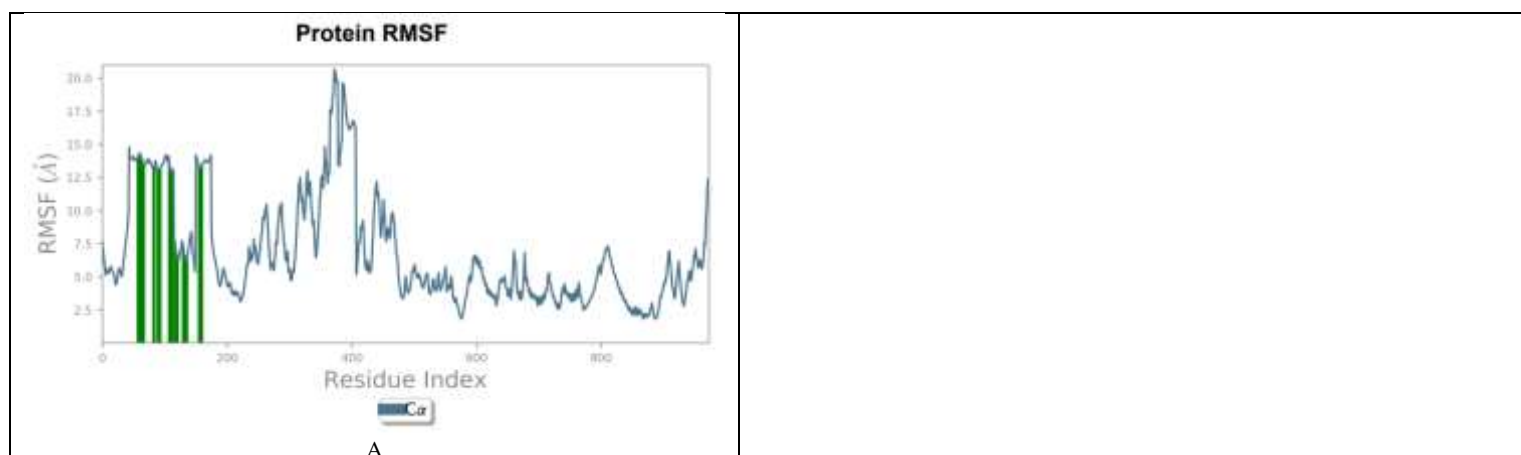
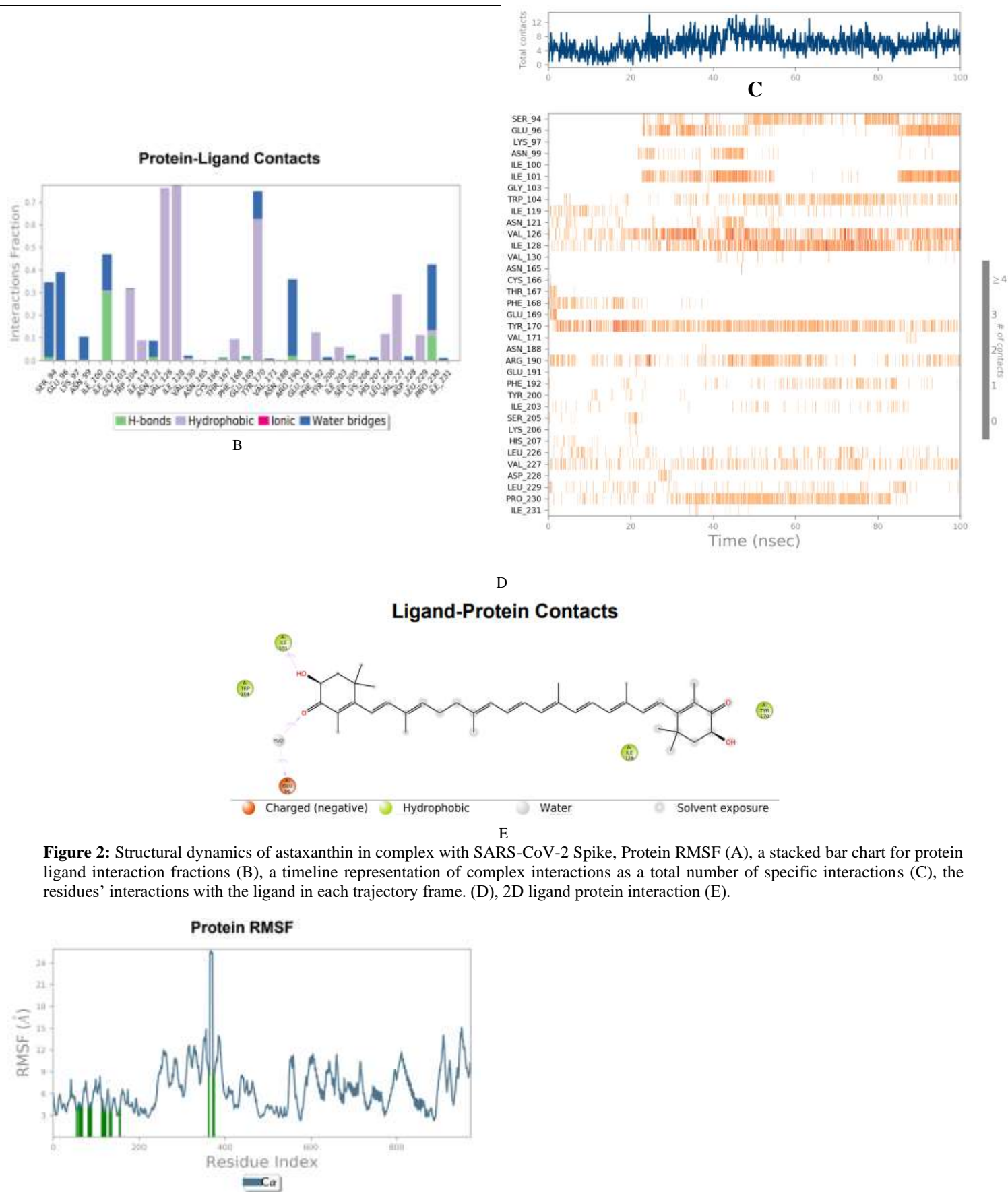


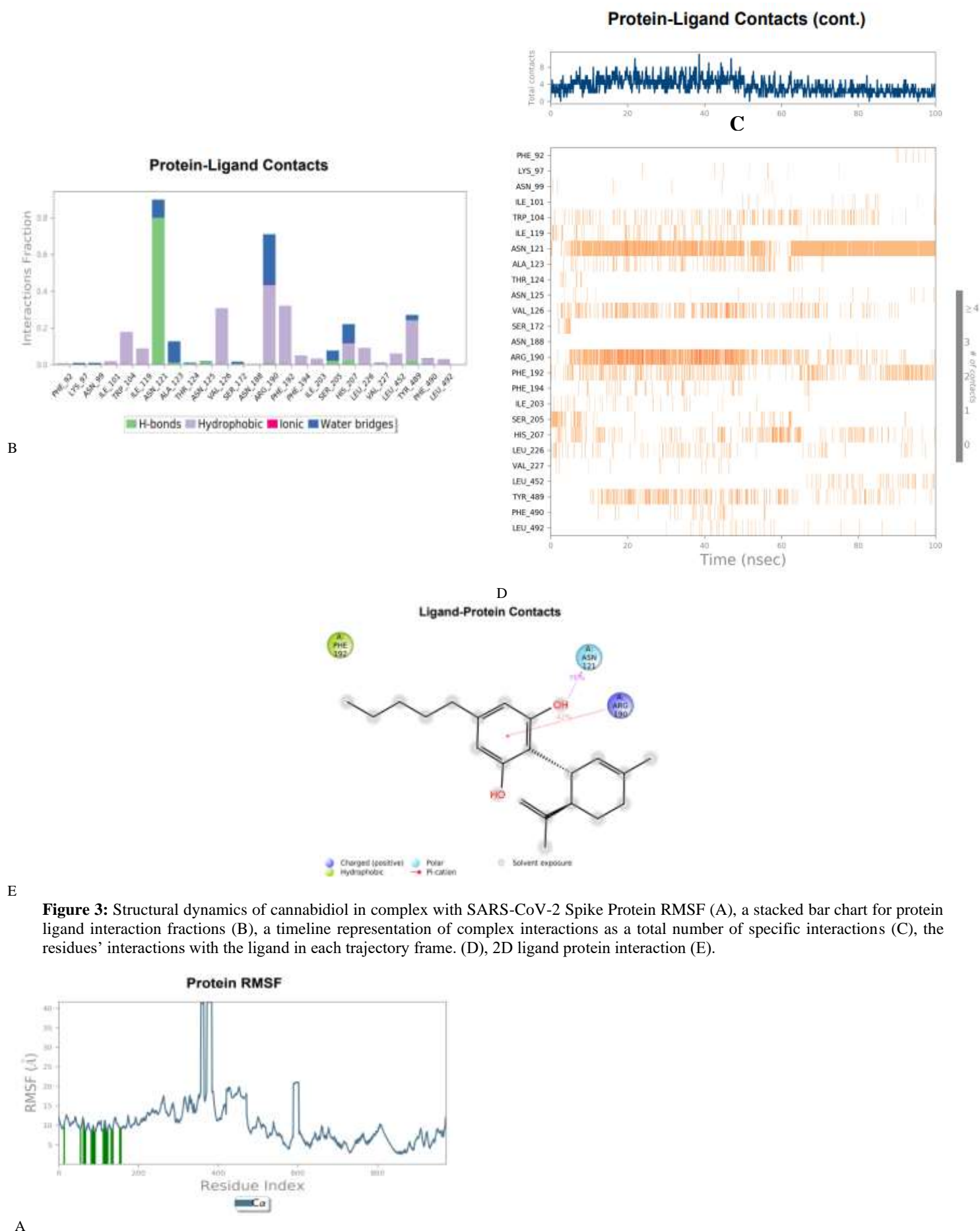
Figure 1: Structural dynamics of 6 ligands; astaxanthin (A), cannabidiol (B), capsaicin (C), cladosin (D), rhodatin (E), and carrageenan (F) bound to SARS-CoV-2 spike glycoprotein (PDB ID. 6VXX), Backbone C α RMSD (in blue) and ligand RMSD (in red) calculated during the 100 ns of MD trajectories

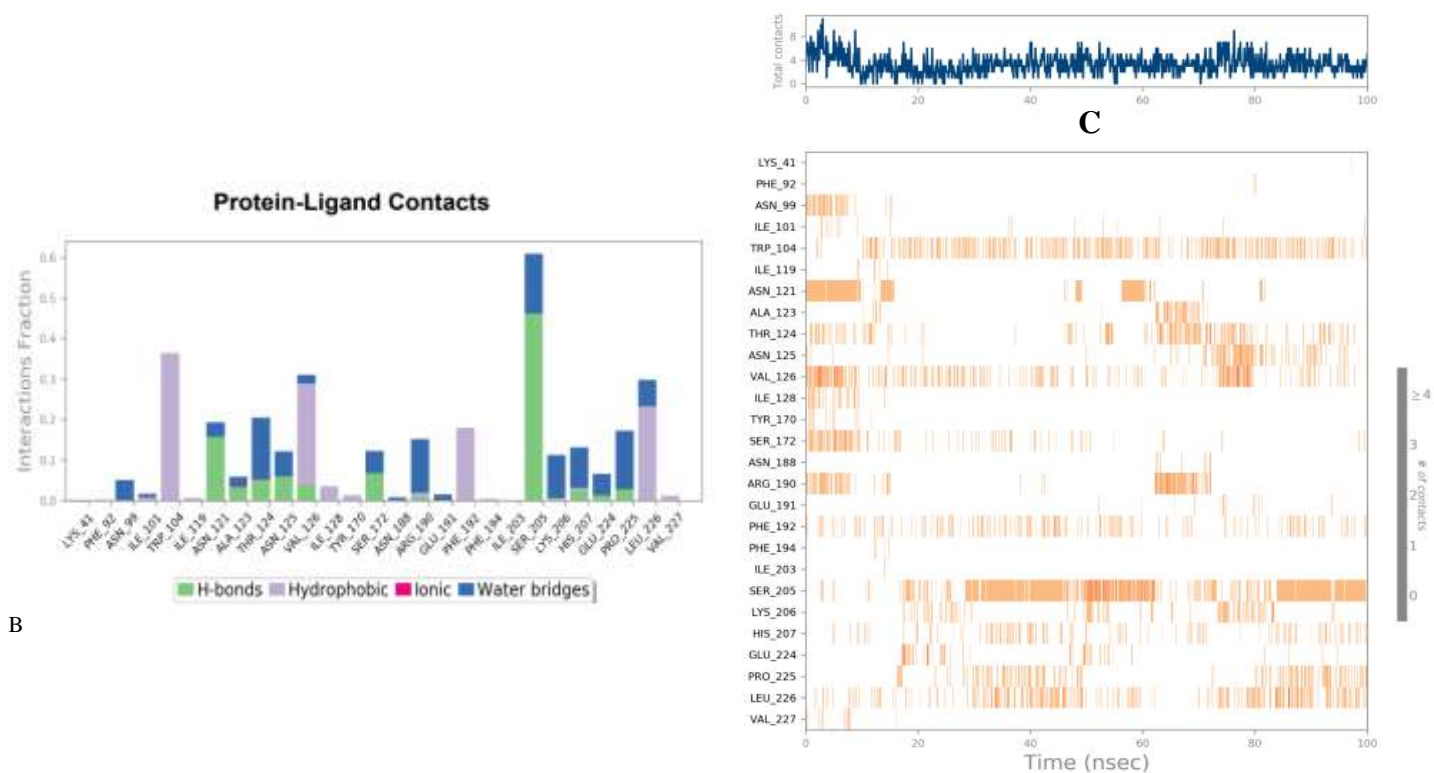




A

Figure 2: Structural dynamics of astaxanthin in complex with SARS-CoV-2 Spike, Protein RMSF (A), a stacked bar chart for protein ligand interaction fractions (B), a timeline representation of complex interactions as a total number of specific interactions (C), the residues' interactions with the ligand in each trajectory frame. (D), 2D ligand protein interaction (E).



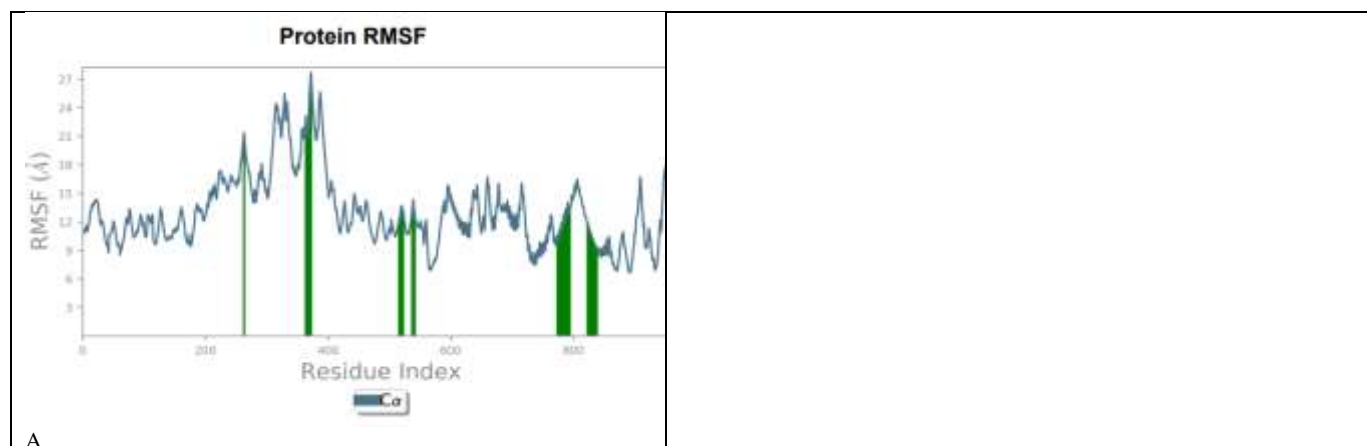


B

D

E

Figure 4: Structural dynamics of capsaicin in complex with SARS-CoV-2 spike, Protein RMSF (A), a stacked bar chart for protein ligand interaction fractions (B), a timeline representation of complex interactions as a total number of specific interactions (C), the residues' interactions with the ligand in each trajectory frame. (D), 2D ligand protein interaction (E).



A

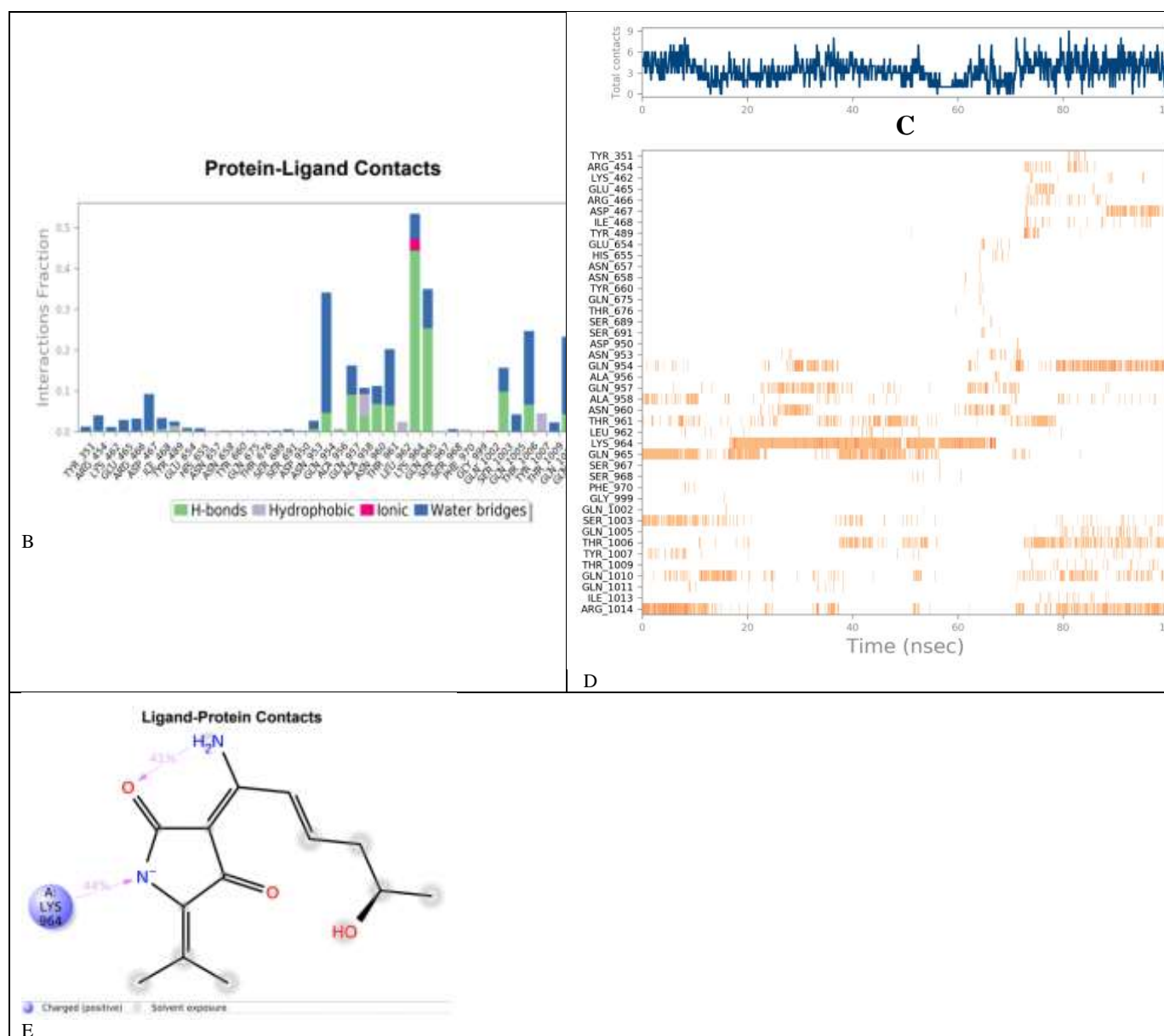
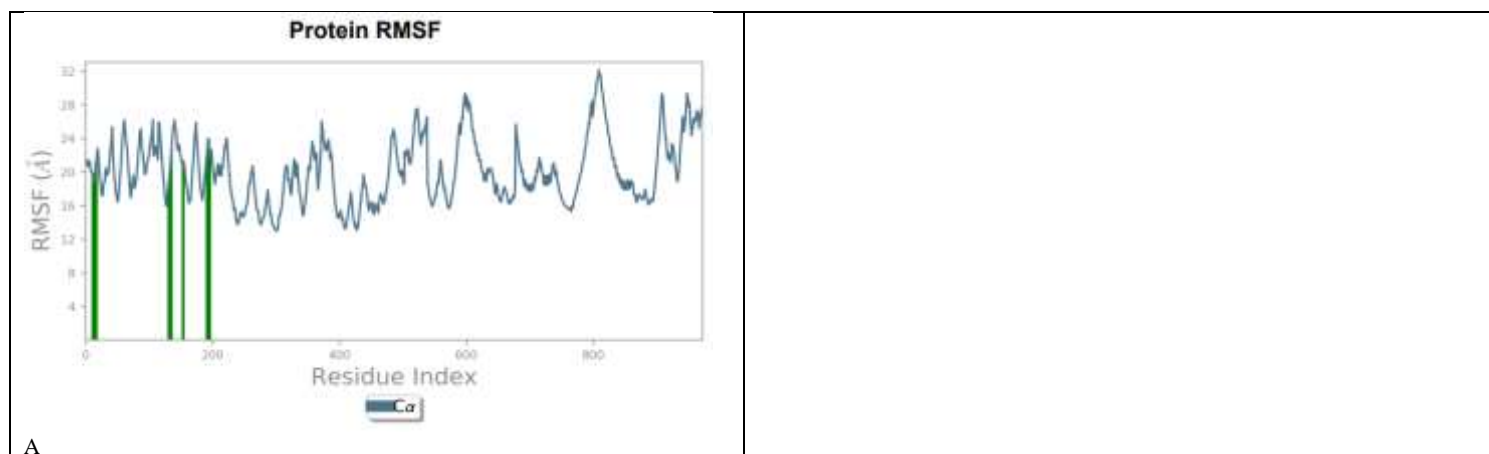


Figure 5: Structural dynamics of cladosin in complex with SARS-CoV-2 spike, Protein RMSF (A), a stacked bar chart for protein ligand interaction fractions (B), a timeline representation of complex interactions as a total number of specific interactions (C), the residues' interactions with the ligand in each trajectory frame. (D), 2D ligand protein interaction (E).



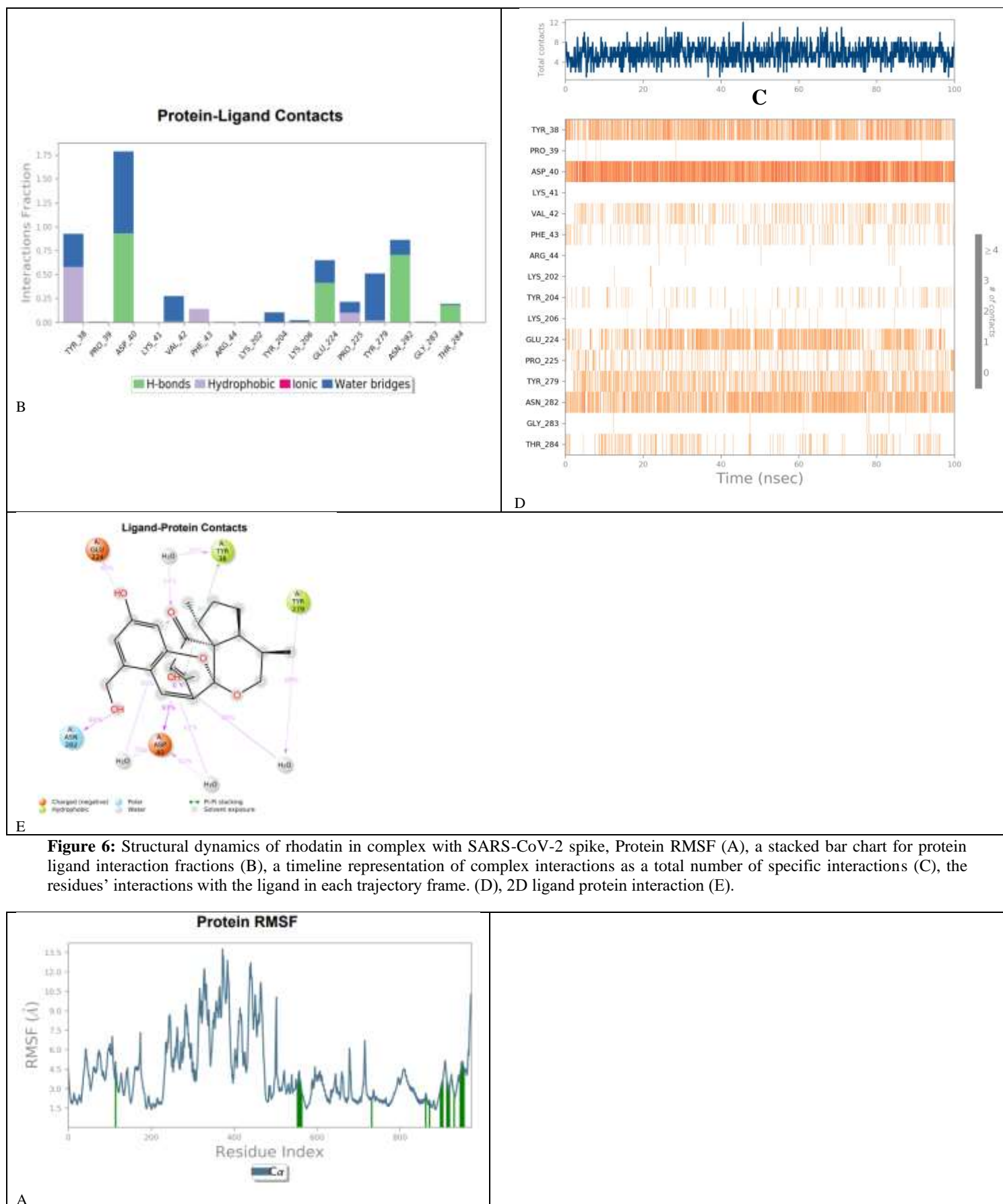


Figure 6: Structural dynamics of rhodatin in complex with SARS-CoV-2 spike, Protein RMSF (A), a stacked bar chart for protein ligand interaction fractions (B), a timeline representation of complex interactions as a total number of specific interactions (C), the residues' interactions with the ligand in each trajectory frame. (D), 2D ligand protein interaction (E).

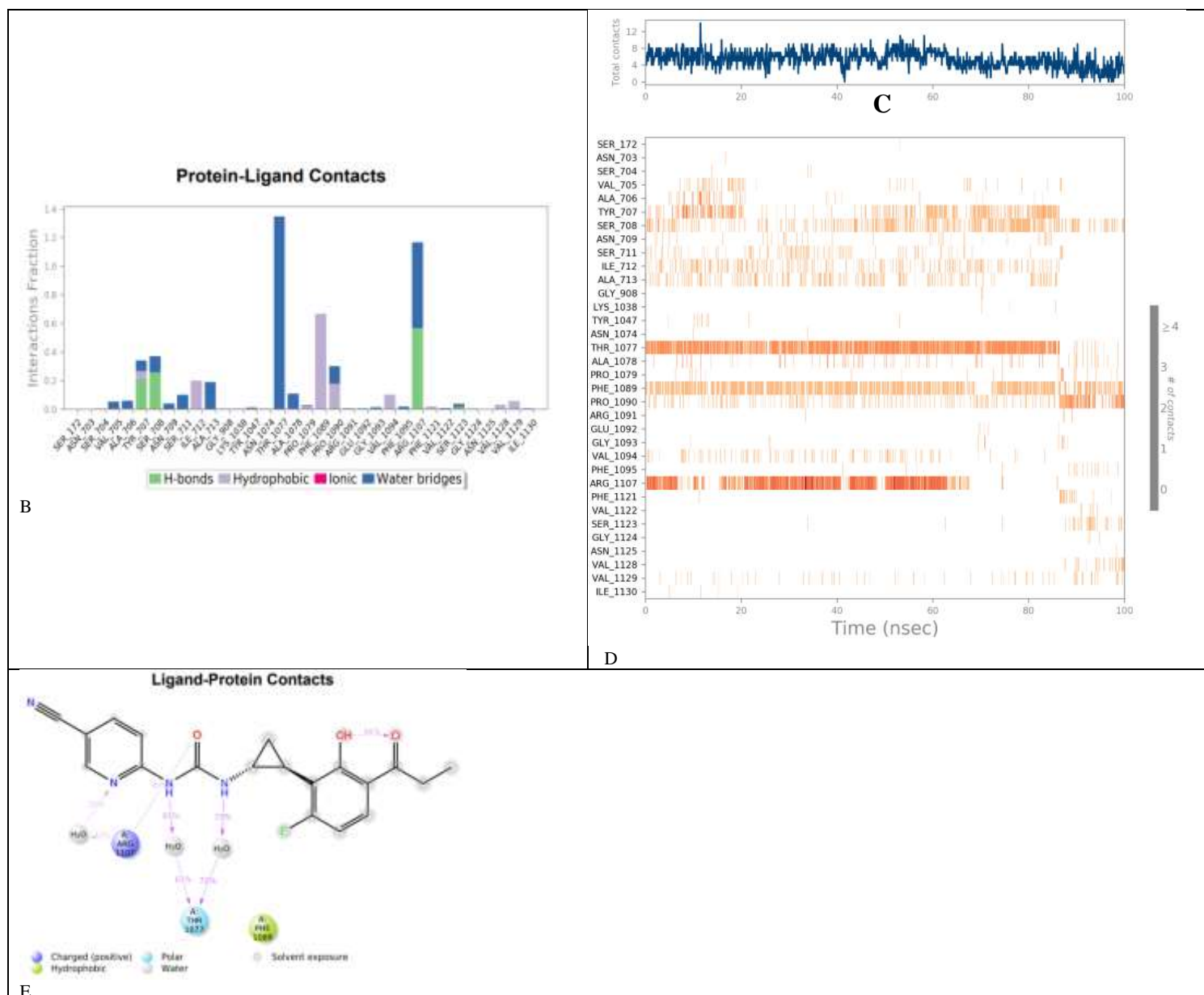


Figure 7: Structural dynamics of carrageenan in complex with SARS-CoV-2 spike, Protein RMSF (A), a stacked bar chart for protein ligand interaction fractions (B), a timeline representation of complex interactions as a total number of specific interactions (C), the residues' interactions with the ligand in each trajectory frame. (D), 2D ligand protein interaction (E).

Carrageenan was observed to engage with the pocket by interacting with Thr 1077, Phe 1089, and Arg 1107, displaying interaction fractions of 1.3, 0.7, and 1.2, respectively (Figure 7.B). The higher interaction fraction of Thr 1077 can be attributed to its capability to establish interactions with two (-NH groups) of the ligand through water bridges. Meanwhile, Arg 1107 demonstrated versatility by forming two types of interactions, namely hydrogen bonds and water bridges, with the oxygen atom in the ligand (Figure 7.E). While these interactions initially appeared promising, they proved to be unstable over time, as most of them were disrupted after approximately 80 ns, as evident in Figure 7.D. This instability was further reflected in the complex RMSF plot, where all the residues exhibited high fluctuations, signifying an unstable binding (Figure 7.A).

Conclusion

In summation, these research outcomes have enhanced the understanding of the stability and interactions inherent to the protein-ligand complex, thereby substantiating the potential of the six identified

molecules as antagonists against the RBM of the viral spike protein. The principal aim of this investigation revolved around making a substantial contribution to the examination of novel naturally occurring antiviral compounds. The overarching objective is to advance these findings into *in vitro* and *in vivo* experiments, with the aspiration that these molecules and natural constituents may serve as a foundation for the innovation and formulation of antiviral agents targeting Coronaviruses. Nonetheless, it is imperative to underscore that further inquiries are necessitated to fully explore the prospective applications of medicinal plants harboring these compounds.

Conflict of Interest

The authors declare no conflict of interest.

Authors' Declaration

The authors hereby declare that the work presented in this article is original and that any liability for claims relating to the content of this article will be borne by them.

References

1. Carabelli AM, Peacock TP, Thorne LG, Harvey WT, Hughes J, Peacock SJ, Barclay WS, De Silva TI, Towers GJ, Robertson DL. SARS-CoV-2 variant biology: immune escape, transmission and fitness. *Nat Rev Microbiol.* 2023; 21: 162-177.
2. Zatlá I, Boublenzá L, Hassaine H. The First Days and Months of the COVID-19 Pandemic. *RRJoMV.* 2022; 12(1): 7-13.
3. Zatlá I, Boublenzá L, Hassaine H. Infection and Viral Pathogenesis of SARS-CoV-2. A Review. *RRJoMV.* 2022; 12(2): 17-23.
4. Li G, Hilgenfeld R, Whitley R, De Clercq E. Therapeutic strategies for COVID-19: progress and lessons learned. *Nat Rev Drug Discov.* 2023; 22: 449-475.
5. Zatlá I, Boublenzá L, Hassaine H. Therapeutic and Preventive Approaches against COVID-19: A Review. *RRJoMV.* 2021; 11(3): 26-33.
6. Wang Z, Wang N, Yang L, Song X-q. Bioactive natural products in COVID-19 therapy. *Front Pharmacol.* 2022; 13: 926507.
7. Holst M, Nowak D, Hoch E. Cannabidiol as a Treatment for COVID-19 Symptoms? A Critical Review. *Cannabis Cannabinoid Res.* 2023; 487-494.
8. Alrasheid AA, Babiker MY, Awad TA. Evaluation of certain medicinal plants compounds as new potential inhibitors of novel corona virus (COVID-19) using molecular docking analysis. *In Silico Pharmacol.* 2021; 9: 10.
9. Takahashi JA, Barbosa BVR, Lima MTNS, Cardoso PG, Contigli C, Pimenta LPS. Antiviral fungal metabolites and some insights into their contribution to the current COVID-19 pandemic. *Bioorg Med Chem.* 2021; 46: 116366.
10. Carbone DA, Pellone P, Lubritto C, Ciniglia C. Evaluation of Microalgae Antiviral Activity and Their Bioactive Compounds. *Antibiotics.* 2021; 10(6): 746.
11. Pettersen EF, Goddard TD, Huang CC, Couch GS, Greenblatt DM, Meng EC, Ferrin TE. *J Comput Chem.* 2004; 13: 1605-12.
12. Lan J, Ge J, Yu J, Shan S, Zhou H, Fan S, Zhang Q, Shi X, Wang Q, Zhang L, Wang X. Structure of the SARS-CoV-2 spike receptor-binding domain bound to the ACE2 receptor. *Nature.* 2020; 581: 215-220.
13. Goodsell DS, Olson AJ. Automated Docking of Substrates to Proteins by Simulated Annealing. *Proteins: Struct. Funct. Genet.* 1990; 8: 195-202.
14. Morris GM, Huey R, Lindstrom W, Sanner MF, Belew RK, Goodsell DS, Olson AJ. Autodock4 and AutoDockTools4: automated docking with selective receptor flexibility. *J. Comput. Chem.* 2009; 16: 2785-91.
15. Trott O, Olson AJ. AutoDock Vina: improving the speed and accuracy of docking with a new scoring function, efficient optimization and multithreading. *J Comput Chem.* 2010; 31: 455-461
16. Schrödinger, E., Schrödinger. Centenary Celebra, 2016.
17. Schrödinger L., DE Shaw Research, New York, Maestro-Desmond Interoperability Tools, Schrödinger New York, NY, USA, 2020.
18. Ferreira LG, Dos Santos RN, Oliva G, Andricopulo AD. Molecular docking and structure-based drug design strategies. *Molecules.* 2015; 20(7): 13384-421.
19. Hildebrand PW, Rose AS, Tiemann JKS. Bringing Molecular Dynamics Simulation Data into View. *Trends Biochem Sci.* 2019; 44(11): 902-913.
20. Rasheed MA, Iqbal MN, Saddick S, Ali I, Khan FS, Kanwal S, Ahmed D, Ibrahim M, Afzal U, Awais M. Identification of Lead Compounds against Scm (fms10) in *Enterococcus faecium* Using Computer Aided Drug Designing. *Life (Basel).* 2021; 11(2).
21. Shivakumar D, Williams J, Wu Y, Damm W, Shelly J, Sherman W. Prediction of Absolute Solvation Free Energies using Molecular Dynamics Free Energy Perturbation and the OPLS Force Field. *J Chem Theory Comput.* 2010; 6(5): 1509-1519.
22. Pollastri MP. Overview on the Rule of Five. *Curr Protoc Pharmacol.* 2010; 49.
23. Douglas EV, Pires TL, Blundell DB. Ascher pkCSM: predicting small-molecule pharmacokinetic properties using graph-based signatures. *J Med Chem.* 2015; 58(9): 4066-4072.
24. Aier I, Varadwaj PK, Raj U. Structural insights into conformational stability of both wild-type and mutant EZH2 receptor. *Sci Rep.* 2016; 6(1): 1-10.